atoms only. The same type of boron–oxygen bond breaking also occurs during the cubic-to-trigonal (rhombohedral) and cubic-to-orthorhombic phase transitions.

The thermal ellipsoids of the tetragonal modification of Cr-Cl are consistent with those in the cubic modification, and also with those in the trigonal and orthorhombic modifications of other boracites. The largest atomic displacements occur with the halogens, and they are nearly isotropic. Those of the metal sites are very anisotropic [Cr(1), $U_{11}/U_{22} = 4{\cdot}88$; Cr(2), $U_{22}/U_{11} = 7{\cdot}41$; Cr(3), $U_{33}/U_{22} = 6{\cdot}00$; Cr(4), $U_{33}/U_{22} = 4{\cdot}73$; Cr(5), $U_{33}/U_{22} = 5{\cdot}59$], the largest displacements occurring perpendicular to the strong metal–halogen bonds, *i.e.* parallel to the weak metal–halogen bonds (Fig. 2).

Finally, tetragonal Cr-Cl is the only known example among boracites that has a non-polar structure at low temperature. As shown in Fig. 4 the $Cr(3)O_4Cl$ groups can be considered as dipoles that are oriented along the tetragonal axis and have opposite signs in neighbouring chains. Such a picture is consistent with the observed antiferroelectric behaviour (Ye, Rivera & Schmid, 1991*b*) and possible occurrence of antiphase domains in the Cr-Cl tetragonal phase (Wondratschek & Jeitschko, 1976).

We wish to acknowledge the help of Mr J. T. Zhao for the useful suggestions about single-crystal refinements. We also thank Drs J.-P. Rivera and Z.-G. Ye for assistance during the domain studies by means of the optical He-flow cryostat and Mr E. Burkhardt for help with mounting the polarizing microscope attachment onto the X-ray diffractometer. This study was supported by the Swiss National Science Foundation.

References

ABRAHAMS, S. C., BERNSTEIN, J. L. & SVENSSON, C. (1981). *J. Chem. Phys.* **75**(4), 1912–1918.
AIZU, K. (1970). *Phys. Rev. B.* **2**, 754–772.
BERSET, G., YVON, K., DEPMEIER, W., BOUTELLIER, R. & SCHMID, H. (1984). *Ferroelectrics*, **56**, 13–16.
BOCHKOV, B. G. & DROZHDIN, S. N. (1975). *Sov. Phys. Crystallogr.* **19**, 811–812.
DEBAERDEMAEKER, T., GERMAIN, G., MAIN, P., TATE, C. & WOOLFSON, M. M. (1987). *MULTAN87. A System of Computer Programs for the Automatic Solution of Crystal Structures from X-ray Diffraction Data.* Univ. of York, England.
DOWTY, E. & CLARK, J. (1973). *Z. Kristallogr.* **138**, 64–99.
FLACK, H. D. (1983). *Acta Cryst.* A**39**, 876–881.
GELATO, L. M. & PARTHÉ, E. (1987). *J. Appl. Cryst.* **20**, 139–143.
HALL, S. R. & STEWART, J. M. (1989). Editors. *XTAL2.6 Users Manual.* Univs. of Western Australia, Australia, and Maryland, USA.
NELMES, R. J. & THORNLEY, F. R. (1974). *J. Phys. C*, **7**, 3855–3874.
NESTEROVA, N. N., PISAREV, R. V. & ANDREEVA, G. T. (1974). *Phys. Status Solidi B*, **65**, 103–110.
SCHMID, H. (1965). *J. Phys. Chem. Solids*, **26**, 937–988.
SCHMID, H. & TIPPMANN, H. (1978). *Ferroelectrics*, **20**, 21–36.
SCHMID, H. & TIPPMANN, H. (1979). *J. Cryst. Growth*, **46**, 723–742.
TOLÉDANO, P., SCHMID, H., CLIN, M. & RIVERA, J. P. (1985). *Phys. Rev. B*, **32**, 6006–6038.
WONDRATSCHEK, H. & JEITSCHKO, W. (1976). *Acta Cryst.* A**32**, 664–666.
YE, Z.-G., RIVERA, J.-P. & SCHMID, H. (1990). *Ferroelectrics*, **106**, 87–92.
YE, Z.-G., RIVERA, J.-P. & SCHMID, H. (1991*a*). Ferroelectrics, **116**, 251–260.
YE, Z.-G., RIVERA, J.-P. & SCHMID, H. (1991*b*). Phase Transitions. In the press.

Acta Cryst. (1991). B**47**, 696–701

Defect Clustering in the Superionic Conductor Lithium Germanium Vanadate

BY I. ABRAHAMS

*Department of Chemistry, Heriot-Watt University, Riccarton, Edinburgh EH*14 4*AS, Scotland*

AND P. G. BRUCE

*Department of Chemistry, University of St Andrews, St Andrews, Fife KY*16 9*ST, Scotland*

(*Received* 1 *September* 1990; *accepted* 15 *April* 1991)

Abstract

The defect structure of $Li_{3{\cdot}5}Ge_{0{\cdot}5}V_{0{\cdot}5}O_4$ has been determined at 298 and 573 K using high-resolution powder neutron and synchrotron X-ray diffraction techniques. The compound is one member ($x = 0{\cdot}5$) of an extensive solid-solution range with the general formula $Li_{(3+x)}Ge_{(x)}V_{(1-x)}O_4$ and belongs to the family of Li^+-ion-conducting solids known as the γ-phases. The structure was refined in the ortho-

0108-7681/91/050696-06$03.00

rhombic space group *Pnma* (No. 62), $Z = 4$, with cell dimensions obtained from neutron data at 298 K of $a = 10{\cdot}8714\,(2)$, $b = 6{\cdot}2606\,(1)$ and $c = 5{\cdot}1258\,(1)$ Å, $V = 348{\cdot}87$ Å^3, $M_r = 150{\cdot}05$, $D_x = 2{\cdot}858$ g cm^{-3}, and at 573 K of $a = 10{\cdot}9326\,(2)$, $b = 6{\cdot}3016\,(1)$ and $c = 5{\cdot}1593\,(1)$ Å, $V = 355{\cdot}44$ Å^3, $D_x = 2{\cdot}805$ g cm^{-3}. The final R factors for the neutron data at 298 K were $R_{wp} = 5{\cdot}33$, $R_{ex} = 2{\cdot}87\%$ and at 573 K $R_{wp} = 4{\cdot}27$, $R_{ex} = 4{\cdot}17\%$. The lithium-rich defects present are based on two structural elements. At 298 K these seem to be combined to form one defect cluster while at 573 K at least two defect clusters must be present. The defects differ from those discussed in previous studies of another γ-solid-solution LISICON, $Li_3Zn_{0.5}GeO_4$.

Introduction

Solids which exhibit fast ionic conduction are of considerable interest for use as solid electrolytes in applications such as batteries and chemical sensors (Takahashi, 1989). High Li^+-ion conductivity is achieved in a number of solids at elevated temperatures, however this imposes limitations on practical applications for devices using such electrolytes. Materials which support appreciable Li^+-ion conductivity at ambient temperatures are therefore of great interest.

A class of Li^+-ion-conducting solids known as the γ-phases have been investigated (Rodger, Kuwano & West, 1985). They consist of interstitial solid solutions, and it is the presence of the interstitial ions which gives rise to high ionic conductivity. The γ-solid solutions may be divided into two main groups. The first group is based on stoichiometric solids such as the γ-polymorph of Li_2ZnGeO_4, with solid-solution formation occurring by the replacement of a Zn^{2+} ion by one Li^+ ion and an additional Li^+ ion being incorporated in an interstitial site. This yields the solid-solution system $Li_{(2+2x)}Zn_{(1-x)}GeO_4$, which is generally known as LISICON. The defect structure of this solid solution has been reported (Abrahams, Bruce, David & West, 1989). The second group is based on solids such as γ-Li_3VO_4; solid-solution formation occurring by replacement of V^{5+} with Ge^{4+} again with introduction of an interstitial Li^+ ion, yielding the solid solution $Li_{(3+x)}Ge_xV_{(1-x)}O_4$. Both γ-Li_2ZnGeO_4 and γ-Li_3VO_4 are essentially isostructural with the γ-polymorph of Li_3PO_4. Not only are the solid-solution mechanisms different for LISICON and the germanium vanadate but their respective conductivities differ markedly at room temperature. LISICON compositions are known to have rather low Li^+-ion conductivities at ambient temperature, of the order of 10^{-7} S cm^{-1}, while those for the lithium germanium vanadates are approximately two orders of magnitude higher. Indeed, $Li_{3.5}Ge_{0.5}V_{0.5}O_4$ (corresponding to the solid-solution composition $x = 0{\cdot}5$) has been found to have a conductivity in excess of 10^{-5} S cm^{-1} at 291 K (Kuwano & West, 1980) which ranks it amongst the best Li^+-ion conductors known at these temperatures and thus suitable for practical applications. Consequently, a detailed knowledge of the Li^+-ion distribution in $Li_{3.5}Ge_{0.5}V_{0.5}O_4$ is of some importance.

Here we report on the defect structure of the superionic conductor $Li_{3.5}Ge_{0.5}V_{0.5}O_4$ at two temperatures. The defect structures have been determined using powder neutron and X-ray diffraction, and differ from those in LISICON.

Experimental

Preparation

$^7Li_{3.5}Ge_{0.5}V_{0.5}O_4$ was prepared by solid-state reaction of appropriate quantities of $^7Li_2CO_3$, GeO_2 and V_2O_5. The reactants were initially ground up as a slurry in ethanol and evaporated to dryness. Reaction was carried out in a gold crucible which was placed in a muffle furnace, initially at 923 K for 12 h followed by 6 h at 1123 K, before quenching to room temperature. Purity was checked by X-ray powder diffraction using a Stöe–Guinier camera.

Diffraction data collection

Synchrotron X-ray powder diffraction data were collected on the 9·1 diffractometer at the Daresbury SRS. The instrument uses a Debye–Scherrer geometry with the sample mounted centrally in a 0·5 mm Lindemann tube which was rotated axially. Data were collected at a constant wavelength of 1·4963 Å, between 10 and 60° in 2θ, using a step-scanning detector with step widths of 0·01°. Rietveld refinement was carried out with the program *MPROF*, version X14·4 (Murray & Fitch, 1989), using a Pearson VII function. Coefficients for calculation of scattering factors were taken from the literature (*International Tables for X-ray Crystallography*, 1974, Vol. IV, p. 99).

High-resolution time-of-flight powder neutron diffraction profiles were collected at 298 and 573 K on the HRPD diffractometer at ISIS, Rutherford–Appleton Laboratory. The sample was mounted 1 m in front of the backscattering detectors and data were obtained spanning the range 20–120 ms. The diffraction profiles were fitted using a modified Rietveld method (David, 1990) with the peak shape modelled by a convolution of a pseudo-Voigt and two exponential functions (David, Ahporiaye, Ibberson & Wilson, 1988). The scattering lengths used were Ge = 0·8193, O = 0·5805, ^{7}Li = −0·220, $V = -0{\cdot}0382 \times 10^{-12}$ cm (Koester & Rauch, 1981).

Structure refinement

A similar approach was taken to the refinement of the structural models for both the 298 and 573 K data sets, that of the 298 K structure is described below.

Initial values for the unit-cell dimensions were obtained by refinement of indexed d spacings measured from the diffraction profile. The atomic parameters of the LISICON (Abrahams *et al.*, 1989) structure were used as a starting model (space group *Pnma*, No. 62, *International Tables for Crystallography*, 1983, Vol. A). In this model Ge and V were assumed to share a tetrahedral site occupied wholly by Ge in LISICON. No lithium ions were included at this stage. The scale and five Chebychev polynomial parameters used to fit the background were varied first, followed in subsequent iterations by the unit-cell dimensions, zero-point correction and the half width of the Gaussian part of the peak shape. With the occupancies of all sites fixed, Ge/V and O positional and isotropic thermal parameters were then varied.

Using the observed and calculated structure factors from the above model a difference Fourier computation was carried out which revealed several strong negative peaks indicative of ^{7}Li. The two strongest peaks at 0·43, 0·75, 0·17 and 0·16, 0·00, 0·32 were in close agreement with two of the framework tetrahedral lithium sites seen in LISICON, and were similarly labelled Li(1) and Li(2) respectively. Refinement of the Li^+-ion positional and thermal parameters on these sites, but with a fixed occupancy of unity on each site, gave large isotropic B factors especially on Li(2). Two sets of tetrahedral sites share common faces with the Li(1) and Li(2) sites, these are labelled Li(1a) and Li(2a) respectively. It is known from the work on LISICON that it is possible for such sites to accommodate Li^+ ions displaced from the Li(1) and Li(2) sites. The centres of the sites labelled (2) and (2a) are in too close proximity to be occupied by lithium simultaneously, and a similar situation pertains for the (1) and (1a) sites. Li^+ ions were introduced into the (2a) site, at first the occupancies of the (2) and (2a) sites were allowed to vary independently: it was observed that the sum of the occupancies of sites (2) and (2a) were unity within e.s.d.'s. Subsequently the occupancy of sites (2) and (2a) were constrained to a total value of one. Refinement of lithium on site (1a) was also attempted; however, this refinement failed to converge. Introducing anisotropic thermal parameters on Li(1) did yield a stable refinement, but with a large B_{33} element indicating that the scattering was distributed along the c axis and towards the (1a) site (Fig. 1). The large value of B_{33} and the modest values of most of the other thermal parameters leads us to conclude that the Li^+ ions in site (1) are positionally disordered. Difference Fourier maps were used to locate the remaining lithiums in two interstitial octahedral sites labelled Li(3) and Li(4). Two further octahedral sites are present in the structure (Abrahams *et al.*, 1989), they were also tested for lithium scattering but refined to give zero or negative occupancies. In the final refinement the total interstitial Li^+ occupancy was fixed at that calculated from the formula; isotropic thermal parameters were refined for all Li^+ ions except Li(1), with those of the two octahedral sites, Li(3) and Li(4), being tied together. It should be noted that the somewhat large B factors of Li(3)/Li(4) at 298 K are unlikely to reflect the thermal vibrations alone and probably also result from positional disorder. Anisotropic thermal parameters were refined for all the heavy atoms.

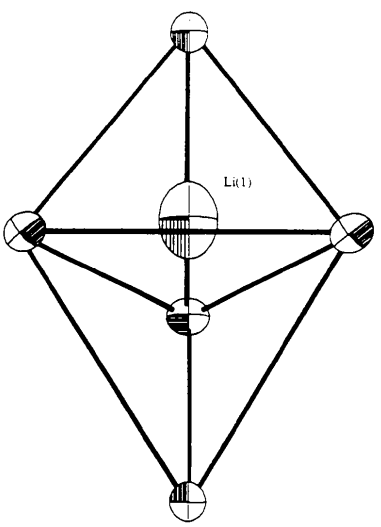

Fig. 1. *ORTEP* plot showing Li(1) surrounded by five oxide ions.

The R factors for the final refinement at 298 K were $R_{wp} = 5{\cdot}33$, $R_{ex} = 2{\cdot}87\%$ and at 573 K, $R_{wp} = 4{\cdot}27$, $R_{ex} = 4{\cdot}17\%$. The fitted profiles are shown in Figs. 2 and 3 and final refined parameters are given in Tables 1 and 2 with bond lengths in Tables 3 and 4.* The profile fits are generally good with that at elevated temperature being marginally superior.

The scattering of neutrons by vanadium is relatively weak when compared with its X-ray scattering factor and we therefore collected synchrotron X-ray data in order to confirm the vanadium occupancy.

* Lists of atomic coordinates, cell parameters, anisotropic thermal parameters, R values, neutron data and synchrotron X-ray diffraction data have been deposited with the British Library Document Supply Centre as Supplementary Publication No. SUP 54175 (87 pp.). Copies may be obtained through The Technical Editor, International Union of Crystallography, 5 Abbey Square, Chester CH1 2HU, England.

The atomic parameters obtained from the neutron refinement were used as a starting model for the parallel refinement using the synchrotron X-ray data at 298 K. Initially only the heavy-atom positional and thermal parameters were allowed to refine, with the rest of the model fixed. In the final refinement the vanadium occupancy was allowed to vary and refined to a value of 0·52 (2), confirming the assumption that the vanadium remains on the tetrahedral site. The R factors for the final refinement were R_{wp} = 10·46, R_{ex} = 5·88, R_I = 4·72%.

Discussion

The structure of $Li_{3\cdot5}Ge_{0\cdot5}V_{0\cdot5}O_4$ is best explained by first considering that of the parent stoichiometric

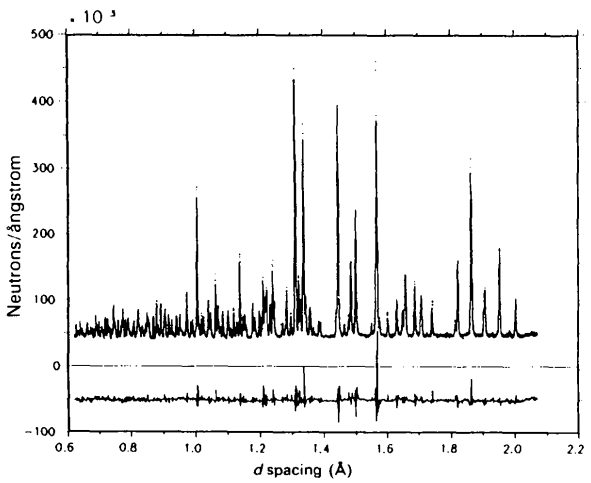

Fig. 2. Fitted powder neutron diffraction profile for $Li_{3\cdot5}Ge_{0\cdot5}V_{0\cdot5}O_4$ at 298 K with observed (points), calculated (line) and difference plots.

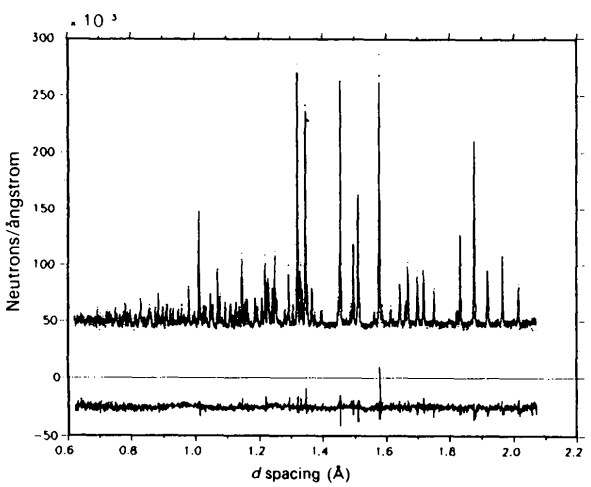

Fig. 3. Fitted powder neutron diffraction profile for $Li_{3\cdot5}Ge_{0\cdot5}V_{0\cdot5}O_4$ at 573 K with observed (points), calculated (line) and difference plots.

Table 1. *Final refined cell and atomic parameters for* $Li_{3\cdot5}V_{0\cdot5}Ge_{0\cdot5}O_4$ *from powder neutron data at* 298 K *with estimated standard deviations in parentheses*

R_{wp} = 5·33, R_{ex} = 2·87%, a = 10·8714 (2), b = 6·2606 (1), c = 5·1258 (1) Å.

	Position	x	y	z	B (Å²)	Occupancy
Ge	4(*c*)	0·4124 (2)	0·25	0·3367 (4)	–	0·5
V	4(*c*)	0·4124 (2)	0·25	0·3367 (4)	–	0·5
O(1)	8(*d*)	0·3371 (1)	0·0250 (2)	0·2196 (2)	–	1·0
O(2)	4(*c*)	0·0869 (2)	0·75	0·1725 (3)	–	1·0
O(3)	4(*c*)	0·0628 (1)	0·25	0·2787 (3)		1·0
Li(1)	4(*c*)	0·4248 (5)	0·75	0·174 (1)	–	1·0
Li(2)	8(*d*)	0·1659 (4)	−0·0049 (7)	0·330 (2)	1·2 (2)	0·76 (3)
Li(2*a*)	8(*d*)	0·169 (2)	0·022 (3)	0·213 (6)	2·2 (4)	0·24 (3)
Li(3)	4(*c*)	0·218 (3)	0·25	−0·028 (5)	4·4 (4)	0·25 (1)
Li(4)	8(*d*)	0·026 (3)	0·533 (6)	0·447 (6)	4·4 (4)	0·126 (6)

Anisotropic thermal parameters

	B_{11}	B_{22}	B_{33}	B_{23}	B_{13}	B_{12}
Ge/V	1·07 (8)	0·93 (9)	1·3 (1)	0·0	−0·42 (9)	0·0
O(1)	0·71 (4)	1·66 (5)	1·74 (5)	−0·43 (4)	0·15 (4)	−0·28 (3)
O(2)	0·91 (6)	1·33 (6)	1·09 (6)	0·0	−0·07 (6)	0·0
O(3)	0·38 (6)	1·15 (6)	1·49 (7)	0·0	−0·24 (5)	0·0
Li(1)	2·1 (2)	2·9 (2)	5·6 (3)	0·0	−1·2 (3)	0·0

Table 2. *Final refined cell and atomic parameters for* $Li_{3\cdot5}V_{0\cdot5}Ge_{0\cdot5}O_4$ *from powder neutron data at* 573 K *with estimated standard deviations in parentheses*

R_{wp} = 4·27, R_{ex} = 4·17%, a = 10·9326 (2), b = 6·3016 (1), c = 5·1593 (1) Å.

	Position	x	y	z	B (Å²)	Occupancy
Ge	4(*c*)	0·4121 (3)	0·25	0·3389 (6)	–	0·5
V	4(*c*)	0·4121 (3)	0·25	0·3389 (6)		0·5
O(1)	8(*d*)	0·3377 (2)	0·252 (2)	0·2228 (3)	–	1·0
O(2)	4(*c*)	0·0881 (2)	0·75	0·1722 (4)	–	1·0
O(3)	4(*c*)	0·0618 (2)	0·25	0·2766 (4)		1·0
Li(1)	4(*c*)	0·4257 (7)	0·75	0·177 (2)	–	1·0
Li(2)	8(*d*)	0·1667 (5)	−0·0049 (8)	0·323 (1)	1·5 (2)	0·75 (2)
Li(2*a*)	8(*d*)	0·163 (2)	0·030 (3)	0·173 (6)	3·3 (7)	0·25 (2)
Li(3)	4(*c*)	0·216 (3)	0·25	−0·027 (7)	2·8 (4)	0·20 (1)
Li(4)	8(*d*)	0·023 (2)	0·537 (4)	0·459 (6)	2·8 (4)	0·152 (6)

Anisotropic thermal parameters

	B_{11}	B_{22}	B_{33}	B_{23}	B_{13}	B_{12}
Ge/V	1·2 (1)	0·8 (1)	1·6 (1)	0·0	0·0 (1)	0·0
O(1)	1·72 (7)	1·69 (7)	2·94 (8)	−0·46 (6)	0·12 (6)	−0·41 (4)
O(2)	1·88 (9)	1·57 (8)	1·65 (9)	0·0	−0·17 (9)	0·0
O(3)	1·00 (8)	1·63 (9)	2·3 (1)	0·0	−0·79 (7)	0·0
Li(1)	3·0 (3)	4·2 (4)	8·9 (5)	0·0	−3·6 (4)	0·0

compound γ-Li_3VO_4 and then describing the formation of the interstitial solid solution from it. γ-Li_3VO_4 consists essentially of hexagonal close-packed oxide ions with the Li^+ and V^{5+} cations filling half the available tetrahedral sites. The tetrahedral sites are arranged in face-sharing pairs, each pair may be considered to be a single trigonal bipyramidal site. Four vacant octahedral sites are also present within the oxygen framework. In γ-Li_3VO_4, VO_4 tetrahedra are isolated from each other and only corner share with LiO_4 tetrahedra which are themselves arranged in groups of three edge-sharing

Table 3. *Interatomic distances* (Å) *for* $Li_{3\cdot5}V_{0\cdot5}Ge_{0\cdot5}O_4$ *at* 298 K *with estimated standard deviations in parentheses*)

		Symmetry transformation
Ge/V—O(1)	1·737 (2) × 2	
Ge/V—O(2)	1·721 (3)	
Ge/V—O(3)	1·739 (3)	
Li(1)—O(1)	1·982 (3) × 2	
Li(1)—O(2)	1·930 (6)	
Li(1)—O(3)	2·031 (5)	
Li(2)—O(1)	1·954 (5)	*x*, *y*, *z*
Li(2)—O(1′)	2·001 (9)	0·5 − *x*, − *y*, 0·5 + *z*
Li(2)—O(2)	1·935 (6)	
Li(2)—O(3)	1·968 (5)	
Li(2*a*)—O(1)	1·83 (2)	*x*, *y*, *z*
Li(2*a*)—O(1′)	2·55 (3)	0·5 − *x*, − *y*, 0·5 + *z*
Li(2*a*)—O(1″)	2·61 (3)	0·5 − *x*, − *y*, 0·5 + *z*
Li(2*a*)—O(2)	1·93 (1)	
Li(2*a*)—O(3)	1·87 (2)	
Li(3)—O(1)	2·30 (2) × 2	*x*, *y*, *z*; *x*, 0·5 − *y*, *z*
Li(3)—O(1′)	2·24 (2) × 2	0·5 − *x*, 0·5 + *y*, 0·5 + *z*;
Li(3)—O(2)	2·62 (3)	0·5 − *x*, − *y*, 0·5 + *z*
Li(3)—O(3)	2·31 (3)	
Li(4)—O(1)	2·25 (3)	0·5 + *x*, 0·5 − *y*, 0·5 − *z*
Li(4)—O(1′)	2·04 (3)	0·5 − *x*, 0·5 + *y*, 0·5 + *z*
Li(4)—O(2)	2·06 (3)	*x*, *y*, *z*
Li(4)—O(2′)	2·91 (3)	− *x*, − *y*, − *z*
Li(4)—O(3)	2·01 (3)	*x*, *y*, *z*
Li(4)—O(3′)	2·18 (3)	− *x*, − *y*, − *z*

Table 4. *Interatomic distances* (Å) *for* $Li_{3\cdot5}V_{0\cdot5}Ge_{0\cdot5}O_4$ *at* 573 K *with estimated standard deviations in parentheses*

		Symmetry transformation
Ge/V—O(1)	1·740 (2) × 2	
Ge/V—O(2)	1·720 (4)	
Ge/V—O(3)	1·742 (4)	
Li(1)—O(1)	1·997 (4) × 2	
Li(1)—O(2)	1·938 (8)	
Li(1)—O(3)	2·07 (1)	
Li(2)—O(1)	1·949 (6)	*x*, *y*, *z*
Li(2)—O(1′)	2·067 (5)	0·5 − *x*, − *y*, 0·5 + *z*
Li(2)—O(2)	1·931 (5)	
Li(2)—O(3)	1·988 (5)	
Li(2*a*)—O(1)	1·92 (3)	*x*, *y*, *z*
Li(2*a*)—O(1′)	2·35 (3)	0·5 − *x*, − *y*, 0·5 + *z*
Li(2*a*)—O(1″)	2·86 (3)	0·5 − *x*, − *y*, 0·5 + *z*
Li(2*a*)—O(2)	1·95 (2)	
Li(2*a*)—O(3)	1·86 (2)	
Li(3)—O(1)	2·33 (2) × 2	*x*, *y*, *z*; *x*, 0·5 − *y*, *z*
Li(3)—O(1′)	2·24 (2) × 2	0·5 − *x*, 0·5 + *y*, 0·5 + *z*;
Li(3)—O(2)	2·64 (3)	0·5 − *x*, − *y*, 0·5 + *z*
Li(3)—O(3)	2·30 (3)	
Li(4)—O(1)	2·27 (2)	0·5 + *x*, 0·5 − *y*, 0·5 − *z*
Li(4)—O(1′)	2·04 (3)	0·5 − *x*, 0·5 + *y*, 0·5 + *z*
Li(4)—O(2)	2·12 (3)	*x*, *y*, *z*
Li(4)—O(2′)	2·89 (3)	− *x*, − *y*, − *z*
Li(4)—O(3)	2·08 (3)	*x*, *y*, *z*
Li(4)—O(3′)	2·13 (3)	− *x*, − *y*, − *z*

sites (Fig. 4). Formation of the solid solution introduces Li^+ ions into the octahedral sites which displace some Li^+ ions into the (2*a*) sites and induces positional disorder on the Li(1) sites.

Diffraction techniques yield directly an average picture of the structure for the solid solution. However, close examination of the data taking into consideration the relative occupancies, positional parameters and the need to minimize Li^+-ion repulsions, strongly suggests a model involving short-range order in which the interstitial Li^+ ions are located in defect clusters. The defect structure for this highly non-stoichiometric solid solution is presented below.

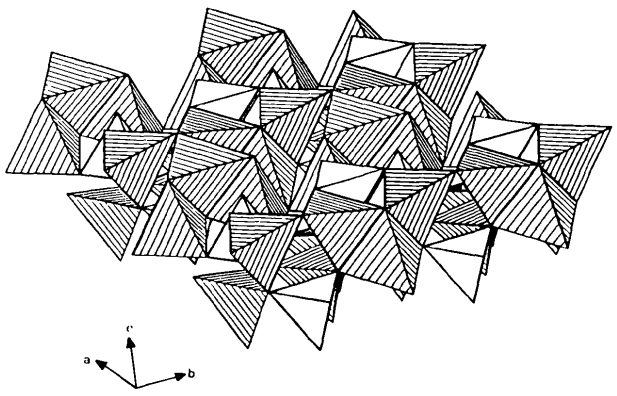

Fig. 4. Structure of stoichiometric γ-Li_3VO_4, in which the cations and their coordinating anions are represented by tetrahedra; shaded and unshaded tetrahedra represent the LiO_4 and VO_4 groups respectively.

Defect structure

The structure of $Li_{3\cdot5}Ge_{0\cdot5}V_{0\cdot5}O_4$ may be described as a domain structure, consisting of homogenously distributed domains with the structure of stoichiometric Li_3VO_4 along with domains of lithium-rich defect clusters. Two basic moieties may be identified from which the lithium-rich defect clusters are built. The first (Fig. 5*a*) consists of an Li^+ ion in site (3) sharing a face with an occupied Li(2) site and another Li(2) site from which the Li^+ ion has been displaced to the neighbouring Li(2*a*) position. It should be noted that the exact location of the (2*a*) position varies with temperature. At 298 K, Li(2*a*) is only just within the site, close to the face shared with the Li(2) site making the ion approximately five-coordinate, while at 573 K the displacement is more pronounced and the ion is closer to the centre of the tetrahedral Li(2*a*) site. The second moiety involves an interstitial Li(4) ion, an Li^+ ion displaced from a (2) to a (2*a*) site, an undisplaced tetrahedral Li(2) ion, and two tetrahedral Li(1) ions (Fig. 5*b*).

At 298 K the ratio of Li(3) and Li(4) ions in each unit cell is approximately 1:1, whereas at 573 K a

ratio of 2:3 is observed. This suggests that at 298 K the moieties combine in pairs to form one larger cluster, in doing so both the Li(2) sites adjacent to Li(3) become vacant (Fig. 6). However, it is not possible to build one cluster which is in accordance with the ratios of Li^+-ion occupancies at 573 K. We therefore propose that while some fusion of the moieties occurs there must be at least two cluster types at this elevated temperature. One probable model for the defect structure at 573 K would involve two clusters, one identical to that at room temperature coexisting with a simple cluster which possesses the structure of the moiety shown in Fig. 5(*b*).

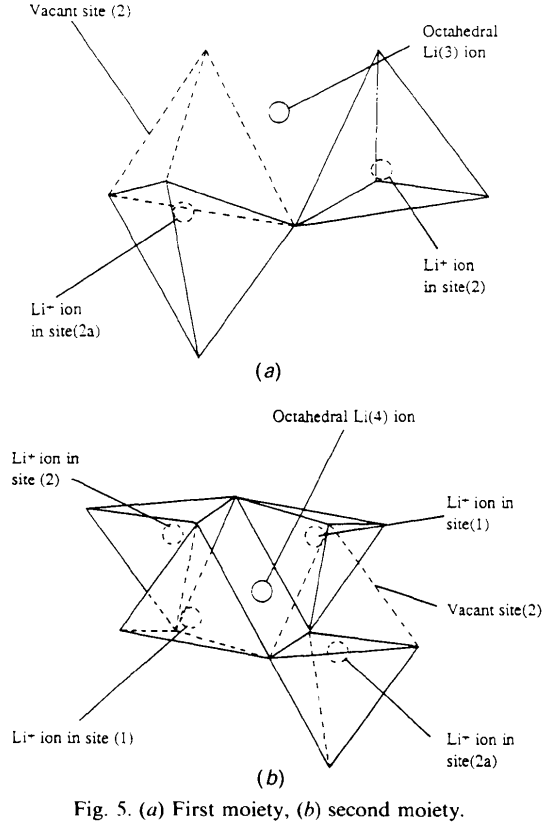

Fig. 5. (*a*) First moiety, (*b*) second moiety.

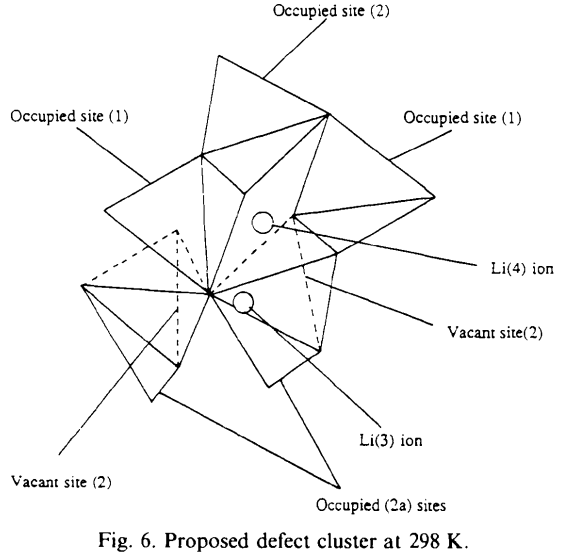

Fig. 6. Proposed defect cluster at 298 K.

Finally, it is interesting to compare the defect structure of the $Li_{3.5}Ge_{0.5}V_{0.5}O_4$ with that of LISICON, $Li_3Zn_{0.5}GeO_4$. The concentration of interstitial Li^+ ions is the same in both cases with half the interstitial octahedral sites being occupied. Similarities do exist between the two γ-solid solutions in that the lithium-rich clusters consist of octahedrally coordinated interstitial Li^+ ions with displacement of Li^+ ions from face-sharing tetrahedral sites. Furthermore, the type I cluster observed in LISICON is very similar to the moiety presented in Fig. 5(*a*). However, the defect clustering present in the two systems is quite distinct with none of the clusters observed in one solid solution appearing in the other, in particular there is no evidence of the type II or III clusters observed in LISICON (Abrahams *et al.*, 1989; Bruce, Abrahams & West 1990) being present in the lithium germanium vanadate.

We wish to thank W. I. F. David and R. M. Ibberson at the Rutherford–Appleton Laboratory for their assistance and the SERC for financial support. PGB is indebted to The Royal Society for a fellowship.

References

ABRAHAMS, I., BRUCE, P. G., DAVID, W. I. F. & WEST, A. R. (1989). *Acta Cryst.* **B45**, 457–462.

BRUCE, P. G., ABRAHAMS, I. & WEST, A. R. (1990). *Solid State Ionics*, **40/41**, 293.

DAVID, W. I. F. (1990). *REFINE*. Time-of-flight refinement program. Rutherford–Appleton Laboratory, England.

DAVID, W. I. F., AKPORIAYE, D. E., IBBERSON, R. M. & WILSON, C. C. (1988). *The High Resolution Powder Diffractometer at ISIS – An Introductory Users Guide*. Version 1.0. Rutherford–Appleton Laboratory, England.

KOESTER, L. & RAUCH, H. (1981). Report 2517/RB. International Atomic Energy Agency, Vienna.

KUWANO, J. & WEST, A. R. (1980). *Mater. Res. Bull.* **15**, 1661–1667.

MURRAY, A. D. & FITCH, A. N. (1989). *Powder Diffraction Program Library (PDPL)*. Univ. College, London, and Univ. of Keele, England.

RODGER, A. R., KUWANO, J. & WEST, A. R. (1985). *Solid State Ionics*, **15**, 185–198.

TAKAHASHI, T. (1989). Editor. *High Conductivity Solid Ionic Conductors – Recent Trends and Applications*. Singapore: World Scientific.